Synthesis of high-pressure hydrous magnesium silicates: Observations and analysis

PAMELA C. BURNLEY* AND ALEXANDRA NAVROTSKY

Center for High Pressure Research and Department of Geological and Geophysical Sciences, Princeton University,
Princeton, New Jersey 08544, U.S.A.

ABSTRACT

Specimens of dense high-pressure hydrous magnesium silicates, notably phase A, phase B, and superhydrous phase B, have been synthesized for use in calorimetric and spectroscopic experiments. X-ray diffraction and electron microprobe analysis were used to study both major and minor phases occurring in the experimental products. We observed the formation of phase A at 16 GPa, 1172 °C; phase B at 15 GPa, 1158 °C; chondrodite at 12 GPa, 1158 °C; and clinohumite at 12 GPa, 1170 °C. These pressures and temperatures are higher than those reported in previous studies. We also observed the formation of phases E and superhydrous B at conditions at which they have been previously observed. However, we propose that there is a high-low transition in superhydrous B. We have not identified phase C in the pressure-temperature-bulk compositional space where it has been observed in previous studies. We conclude that this phase may be identical with superhydrous B, as previously suggested, or that in some studies a humite may have been misidentified as phase C.

INTRODUCTION

Water plays a key role in crustal and surface geology, but little is known about its role in the Earth's deep interior. To be able to predict the importance of H_2O in the mantle we must learn about the ability of mantle minerals to contain H as a function of pressure and temperature, either dissolved in nominally anhydrous minerals or as a component in hydrous phases. For many years it was thought that the mantle was anhydrous, in part because known hydrous phases react to form anhydrous assemblages with increasing pressure and temperature. However, we now know that, in addition to some K-rich amphiboles [stable to 14 GPa at temperatures <1200 °C (Trønnes et al. 1988; Trønnes 1990)], phlogopite [a mica stable to 7 GPa at <1200 °C (Sudo and Tatsumi 1990)], and lawsonite [a hydrous calcium aluminum silicate stable to about 13 GPa at <800 °C (Pawley 1994)], there are many hydrous phases within the $MgO-SiO_2-H_2O$ system with mantle-pressure stabilities, some ranging as high as 20 GPa (Ringwood and Major 1967; Gasparik 1993). In addition, anhydrous minerals such as olivine, pyroxene, and in particular wadsleyite [β-$(Mg,Fe)_2SiO_4$] can contain significant amounts of H_2O (Smyth et al. 1991; Young et al. 1991; Bell and Rossman 1992; Smyth 1994; Inoue et al. 1995). It is also possible that H_2O, once evolved in dehydration reactions, may not be as mobile as previously envisioned (Selverstone et

al. 1992). High-pressure hydrous magnesium silicates constitute a potential reservoir for H_2O in the mantle and a vehicle for carrying subducted H_2O deep into the mantle. Because subduction of hydrated crust could recycle an amount of H_2O equivalent to several oceans back into the mantle over geologic time, subducted H_2O may be an important component of the planet's volatile budget (Peacock 1990).

The presence of hydrous phases would have a significant effect on the mantle. These phases have different physical properties and a different Mg/Si ratio than the bulk mantle. Their presence would tend to increase the modal amount of phases that have complementary composition. For example, it has been suggested that superhydrous phase B (sB) could stabilize stishovite or increase the proportion of pyroxene (Gasparik 1993). As the descending slab is heated these phases would eventually dehydrate; endothermic dehydration reactions could locally depress the geotherm, or the H_2O released could cause melting if it moves out of the slab. H_2O released by dehydration would change the kinetics of slab processes as well as the physical properties of the slab, including electrical conductivity, seismic attenuation, and rheology. In addition, by lowering the effective pressure, H_2O could facilitate brittle fracture and seismicity as it does in the crust (Raleigh and Paterson 1965; Meade and Jeanloz 1991).

At least nine known hydrous magnesium silicates have significant high-pressure stability fields (Fig. 1 and Table 1). Which of these phases could participate in mantle assemblages depends primarily on the equilibrium phase relations between them and the nominally anhydrous
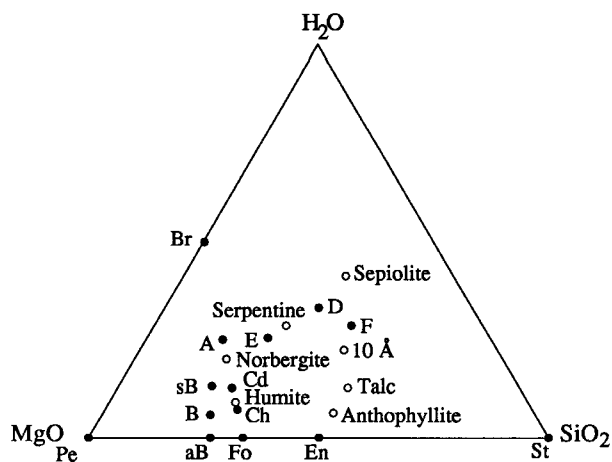

FIGURE 1. Compositional plot of the MgO-SiO$_2$-H$_2$O system. Abbreviations are listed in Table 1. Phases with significant high-pressure stability fields are shown as solid symbols. If these phases are stable in the presence of olivine and pyroxene, they may be part of hydrous mantle assemblages.

mantle minerals. Currently, although high-pressure synthesis delineates the pressure-temperature regions in which these phases can be made (Ringwood and Major 1967; Yamamoto and Akimoto 1974, 1977; Akaogi and Akimoto 1980; Akimoto and Akaogi 1980; Liu 1987; Gasparik 1990, 1993; Kanzaki 1991; Wunder and Schreyer 1992), the thermodynamic properties of these phases are not known, and virtually nothing is known about the equilibrium phase relations because of the lack of reversed experiments. It is also unclear if there are more phases yet to be discovered and if all the known phases have true thermodynamic stabilities [e.g., the 10 Å phase may be metastable (Wunder and Schreyer 1992)]. To learn more about this system we synthesized samples of phase A (A), phase B (B), and sB for calorimetric and spectroscopic measurements. In this paper we report on the synthesis experiments and observations we made in the process of developing a synthesis technique to produce samples suitable for calorimetric study of heats of formation (to be presented later).

METHODS

The synthesis experiments were conducted in the USSA 2000 uniaxial split-sphere apparatus at SUNY Stony Brook. Eight tungsten carbide cubes with 7.5 or 8 mm truncations were used to generate pressure in a 14 mm semisintered MgO octahedron. The sample assemblies followed the basic design of Gwanmesia and Liebermann (1992). Several furnace assemblies were used during the course of this study, all similar in design to the 14-7.5 KG used by Gwanmesia and Liebermann (1992) and the 14-7.5 TL of Gwanmesia et al. (1993). Because of the box design, these furnaces allow for large samples (~40 mg) and produce relatively small temperature gradients. Gwanmesia and Liebermann (1992) measured a gradient of 15 °C/mm from sample center to edge for the 14-7.5 KG furnace; our minor modifications may have increased the gradient but not by more than a factor of two [see data of Burnley (1995)].

Synthesis experiments were conducted both with and without thermocouples. Temperature was measured using a W3%Re vs. W25%Re thermocouple (type D) with the junction formed on the capsule surface to ensure that the temperature measured was that of the sample. The W-Re wires were calibrated at room pressure; we estimate that total uncertainty associated with the use of the wire is ±5 °C. This and the observed temperature-control variations are included in the error given in Table 2. Estimates of the temperature gradient and the effect of pressure on emf (currently not known) are not included in this uncertainty. For experiments without thermocouples, temperature was estimated from the power consumed by the furnace, which was calibrated in other experiments with identical furnace assemblies that contained a thermocouple. Temperature uncertainties quoted for these experiments reflect observed variations among calibration experiments. Experiments were quenched by turning off the power to the furnace. Temperatures dropped to <300 °C within 2 s. Pressure was released slowly overnight.

After the sample capsule was removed from the assembly it was sliced in half using a diamond wafering saw. One-half of the sample was powdered for X-ray diffrac-

TABLE 1. Phases in the system MgO-SiO$_2$-H$_2$O with significant high-pressure stability fields

Name (Abbrev.)	Formula	Ref.
Phase A (A)	Mg$_7$(SiO$_4$)$_2$(OH)$_6$	Horiuchi et al. 1979
Phase B (B)	Mg$_{12}$Si$_4$O$_{19}$(OH)$_2$	Finger et al. 1989
Anhydrous phase B (aB)	Mg$_{14}$Si$_5$O$_{24}$	Finger et al. 1989
Superhydrous phase B (sB)	Mg$_{10}$Si$_3$O$_{14}$(OH)$_4$	Pacalo and Parise 1992
Phase D (D)	MgSiO$_2$(OH)$_2$	Liu 1987
Phase E (E)	Mg$_{2.3}$Si$_{1.25}$H$_{2.4}$O$_6$	Kanzaki 1991
Phase F (F)	Mg$_{1.2}$Si$_{1.9}$H$_{2.4}$O$_6$	Kanzaki 1991
OH–end-member clinohumite (Ch)	Mg$_9$Si$_4$O$_{16}$(OH)$_2$	Yamamoto and Akimoto 1977
OH–end-member chondrodite (Cd)	Mg$_5$Si$_2$O$_8$(OH)$_2$	Yamamoto 1977
Brucite (Br)	Mg(OH)$_2$	
Forsterite (Fo), β-Mg$_2$SiO$_4$ (β), γ-Mg$_2$SiO$_4$	Mg$_2$SiO$_4$	
Enstatite (En), ilmenite, perovskite	MgSiO$_3$	
Stishovite (St)	SiO$_2$	
Periclase (Pe)	MgO	

TABLE 2. Experimental results

Expt., mix	Oil P (bars)	P (GPa)	T (°C)	t (min)	Phases present	Coexisting phases
				Superhydrous phase-B bulk composition		
1496, sB#2	600*	16(1.0)	1000(6)	30	sB, St, Br, Pe	
1561, sB#2	600*	16(1.0)	1059(7)	120	sB, A, *Pe, Mg*	
1660, sB#3	600*	16(1.0)	995(33)**	120	A, sB	
1725, sB#3	590	15.2(1.0)	1154(15)	123	sB, *Pe*, fl	
1790, sB#4	602	15.5(1.0)	1172(40)**	127	sB, A, E, fl	A-E
1857, sB#4	593	15.2(1.0)	1158(6)	122	sB, A, E, fl	sB-A, sB-E
1875, sB#4	605	15.5(1.0)	1129(6)	60	sB, A, E, fl	
1881, sB#5	590	15.2(1.0)	1158(40)**	72	sB, B	sB-B
				Phase-B bulk composition		
1564, B#1	410*	13(1.0)	1278(44)**	1	B, *Fo*	
1659, B#2	550	14.8(1.0)	1000(34)**	120	sB, β	
1669, B#2	400	12.4(1.0)	1000(34)**	120	A, B, Fo, *Br, Pe*	A-B, B-Fo, A-Fo, A-Br, Br-Pe, B-Br
1729, B#2	377	11.8(1.0)	1170(20)	125	B, *Pe, Ch*	B-Ch, B-Pe
1747, B#3	400	12.4(1.0)	1158(25)	13	B, *Cd, Fo*	B-Cd, B-Fo
1752, B#3	400	12.4(1.0)	1154(20)	127	B, *Fo, Cd*	
1758, B#3	400	12.4(1.0)	1154(7)	134	B, *Fo*	
1759, B#3	400	12.4(1.0)	1103(37)**	124	B, *Fo*	
1817, B#4	386	12.0(1.0)	1158(10)	121	B, *Cd, A, Pe*	A-Pe, A-B, B-Cd
1864, B#4a	386	12.0(1.0)	1155(15)	123	B, *Cd, Ch, A*	B-Cd, B-Ch
1876, B#4a	395	12.2(1.0)	1158(10)	120	B, *Cd, A*	B-A, B-Cd
				Phase-A bulk composition		
1774, A#1	304	10.2(1.0)	1091(15)	6	A, *Cd, Br*, fl	
1783, A#1	300	10.0(1.0)	1050(6)	124	A, *Cd, Pe, Br*, fl	A-Cd, A-Pe
1794, A#1	300	10.0(1.0)	1038(36)**	124	A, *Pe, Cd, Br*, fl	A-Br
1830, A#1	291	9.7(1.0)	1050(7)	120	A, *Cd*, fl	
1841, A#1	298	9.8(1.0)	1052(15)	129	A, *Pe*, fl	
				Anhydrous phase-B bulk composition		
1811, aB#2	604	15.5(1.0)	1394(6)	71	aB, β	

Note: Truncation length is 8 mm unless otherwise noted. Ram force can be calculated from oil pressure by multiplying by ram area, which is 0.1075 m². Abbreviations in addition to those listed in Table 1: Mg = magnesite, fl = fluid, sB#2 and sB#3 = $3Mg(OH)_2 + 7MgO + 3SiO_2$, sB#4 = $3Mg_2SiO_4 + 4Mg(OH)_2$, sB#5 = $3(aB\#2) + 4Mg(OH)_2$, B#1 and B#2 = $11MgO + Mg(OH)_2 + 4SiO_2$, B#3 = $4(aB\#2) + 4Mg(OH)_2$, B#4 = B#3 + minor [MgO + $Mg(OH)_2$], B#4a = B#4 + minor [MgO + $Mg(OH)_2$], A#1 = $2Mg_2SiO_4 + 3Mg(OH)_2 + H_2O$, and aB#2 = $5Mg_2SiO_4 + 4MgO$. Minor phases are listed in italics.
* 7.5 mm truncation.
** No thermocouple, temperature estimated from furnace power.

tion and the rest was polished and mounted in Crystal Bond resin for microprobe analysis. Backscattered electron (BSE) micrographs were taken of each bisected sample, providing a method for observing the spatial relationships among phases. The various phases were significantly different in density and therefore could be distinguished by the contrast level in BSE images. The microprobe was used to identify several grains at each BSE contrast level, and then the images were used to study grain relationships and the distribution of phases in the capsule. In choosing grains for microprobe analysis, an effort was made to pick grains that shared grain boundaries with other grains that had already been analyzed. Thus, a catalog of grain-touching-grain relationships was compiled. In addition, with the exception of minor phases, phase identification was confirmed by powder X-ray diffraction.

Synthesis experiments lasted for 2 h. Our goal was to synthesize pure-phase samples of A, B, and sB. To accomplish this we used starting mixtures with the same bulk composition as the desired phase or, in the case of phase A and sB, that phase plus H_2O. However, most experiments contained mixtures of phases. In particular,

we found that refractory starting materials such as quartz and periclase led to incomplete reaction. Even with starting materials 5 μm in size, refractory materials were trapped in growing product crystals and failed to react further. To obtain complete reaction we used fine-grained forsterite (Mg_2SiO_4) and microcrystalline brucite to the maximum extent possible, eliminating or minimizing the amount of refractory material used. Our best results were obtained using the following mixtures: forsterite and brucite (sB#3) for synthesis of sB; forsterite, brucite, and periclase (B#4a) for synthesis of B; and forsterite, brucite, and distilled water (A#1) for synthesis of A. The majority of the experiments contained the target phase as the major phase; however, the formation of accessory phases was inevitable, probably because of small weighing errors and the compositional proximity of many of the hydrous phases. For calorimetric samples accurate quantification of the amount of minor phases is critical. We chose to determine the modal analysis of calorimetric samples (results will be presented elsewhere) by point counting on BSE images of the polished half capsules. For this reason, we synthesized B using a bulk composition slightly richer in H_2O and MgO than that of B to ensure that the minor
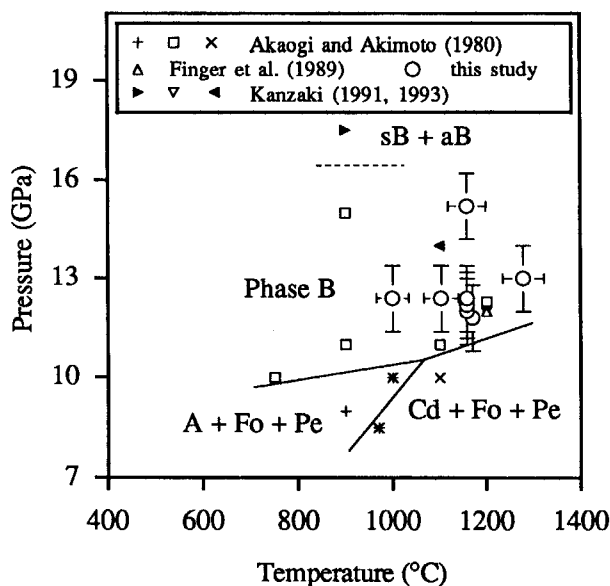
FIGURE 2. Synthesis diagram for phase B. Data from previous studies are also shown. Open symbols indicate the presence of B. Solid symbols, plus signs, and Xs indicate conditions at which phase B did not form. Solid right-pointing triangle represents assemblage aB + sB, solid left-pointing triangle indicates sB replacing B as the breakdown product of A (Kanzaki 1993). Solid lines are phase boundaries from Akaogi and Akimoto (1980). Dashed boundary indicates approximate position of high-pressure decomposition reaction. Experimental uncertainties associated with our pressures and temperatures are shown as error bars. Previous work would have similar or larger experimental uncertainties.
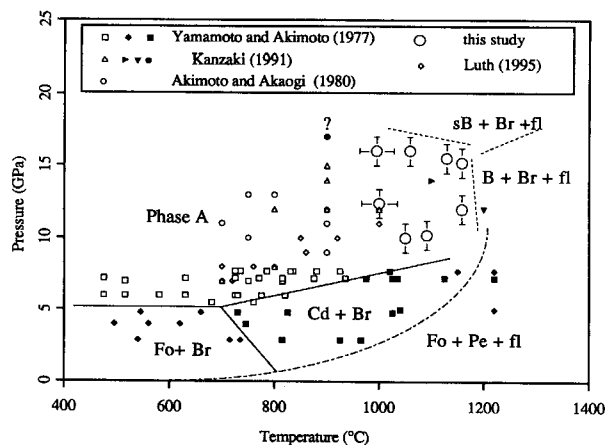

FIGURE 3. Synthesis diagram for phase A. Open symbols indicate presence of A, solid symbols show the presence of assemblages that replace A. Duplicate data points are not plotted for clarity. Data from previous studies are also shown. At low pressures, the fields are labeled according to the assemblages observed. Solid lines are phase boundaries from Yamamoto and Akimoto (1977). Dashed lines at high pressure and high temperature indicate our approximate placement of the breakdown reactions proposed by Kanzaki (1991, 1993). Locations of high-pressure invariant points are not known and therefore not shown. Right-pointing triangle = sB + Br + fl, inverted triangle = B + Br + fl, solid circle = sB + aB + F + fl. The question mark above 16 GPa indicates that the high-pressure breakdown reaction for phase A is not known. Dot-dash curve, representing the approximate position of Br dehydration (Johnson and Walker 1993), is given as a reference. Experimental uncertainties associated with our pressures and temperatures are shown as error bars.

phase was A rather than forsterite, which cannot be distinguished from B in BSE images. Several types of capsules (folded rhenium, folded platinum, and welded platinum) were used. To contain water as a phase, particularly at <16 GPa, it is necessary to use arc-welded capsules; therefore, all our experiments, with the exception of nos. 1496, 1561, and 1564, used welded platinum capsules.

The cell pressure generated by the 8 mm truncations was calibrated using the equilibria between quartz-coesite (1600 °C), CaGeO$_3$ (1000 °C), coesite-stishovite (at 1200 and 2000 °C), and α-β Mg$_2$SiO$_4$ (1200 °C) (Leinenweber, personal communication). Pressures generated by the 7.5 mm truncations were estimated using the calibration of Gwanmesia and Liebermann (1992).

RESULTS

The results of the synthesis experiments are listed in Table 2. The table gives the phases present in each experiment as well as observations regarding phase coexistence.

Phase B formed in experiments at 12–16 GPa and 1000–1278 °C (Fig. 2). It formed small, 1–5 μm, subhedral equant crystals. In phase-B bulk-composition exper-

iments, water was not present as a separate phase; all phases in these experiments were <100 μm.

Phase A formed in experiments at 1000–1172 °C and 10–16 GPa (Fig. 3). In experiments in which H$_2$O was present as a free fluid phase, A formed large (~100 μm), rounded, irregular anhedral crystals. In experiments in which water was not present as a phase, A formed 10 μm equant grains that were subhedral to anhedral. In one experiment (1790), A was found in an intimate mixture with E.

Superhydrous phase B formed in experiments at 1000–1172 °C and 15–16 GPa. In the presence of a free fluid phase, it formed large (100 × 400 μm) subhedral interlocking prisms. In the absence of water as a free phase, it formed 2–10 μm equant anhedral grains. The structure of sB was first refined by Pacalo and Parise (1992) using a crystal synthesized at 1400 °C and 20 GPa. A second refinement by Kudoh et al. (1993), using sB synthesized at 1000 °C and 17 GPa, found a slightly smaller unit cell. The smaller cell ($P2_1nm$) also lacks the center of symmetry of the cell used by Pacalo and Parise ($Pnmn$). The powder patterns from the sB synthesized in this study are better matched by a powder pattern synthesized using the
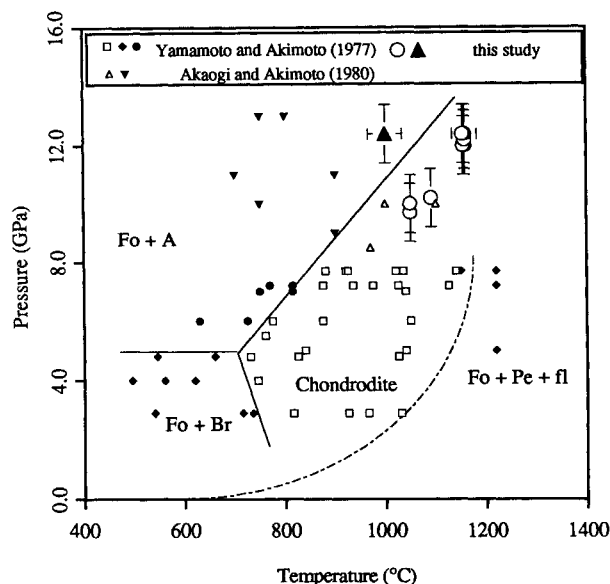
FIGURE 4. Synthesis diagram showing conditions at which chondrodite was observed to form. Data from previous studies are also shown. Open symbols indicate the presence of chondrodite, solid symbols indicate the presence of assemblages that replace it. Fields are labeled according to assemblages observed. Reactions drawn as solid lines are based on those of Yamamoto and Akimoto (1977) but extend into the pressure range of our experiments. The dot-dash curve representing the approximate position of Br dehydration (Johnson and Walker 1993) is given as a reference. Experimental uncertainties associated with our pressures and temperatures are shown as error bars.
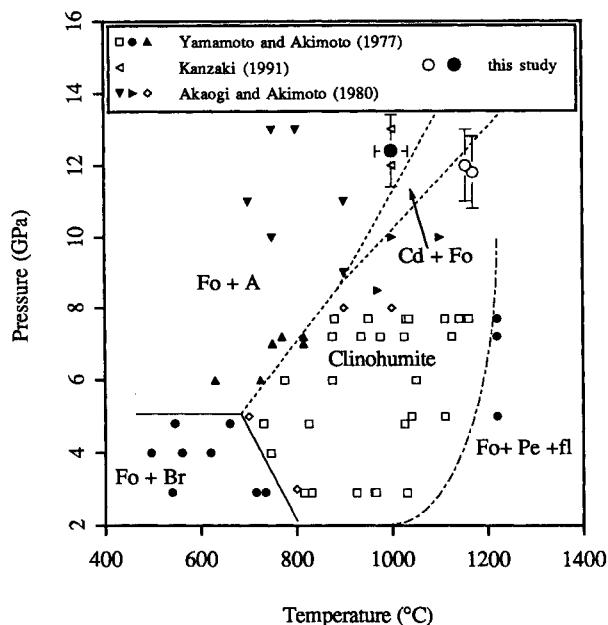

FIGURE 5. Synthesis diagram showing conditions at which clinohumite was observed to form. Data from previous studies are also shown. Open symbols indicate the presence of clinohumite, solid symbols indicate the presence of assemblages that replace it. The fields are labeled according to the assemblages observed. Triangles and inverted triangles = Fo + A and right-pointing solid triangles = Cd + Fo. Reactions drawn as solid lines are from Yamamoto and Akimoto (1977). The dashed lines indicate the proposed locations of the reactions Ch = Fo + A, Cd = Fo + A, and Ch = Cd + Fo. The dot-dash curve representing the approximate position of Br dehydration (Johnson and Walker 1993) is given as a reference. Experimental uncertainties associated with our data are shown as error bars.

unit cell and atomic positions of Kudoh et al. (1993). It is possible that both a "high" and a "low" form of sB exist, with stability fields that are a function of temperature.

Phase E formed in three experiments at 1129–1172 °C and 16 GPa. In one experiment it consisted of 5–10 μm equant crystals mixed intimately with A. In the other experiments it formed elongate (100–200 × 50 μm) euhedral to subhedral tabular crystals growing in radial sprays from the capsule wall.

Chondrodite formed in experiments conducted at 1038–1158 °C and 10–12 GPa (Fig. 4). Clinohumite formed in experiments conducted at 1155 and 1170 °C and 12 GPa (Fig. 5). They both formed 5–10 × 50 μm plates and flakes with one prominent cleavage if the matrix was B and rounded anhedral inclusions if the matrix was A.

With the exception of three experiments discussed below (1790, 1857, and 1875), the distribution of phases in the sample capsules was homogeneous from end to end, and the phases were well mixed. Without exception, all phases were well crystallized. The majority of experiments contained only three phases. In experiments containing brucite, periclase, or both, these phases were present as inclusions and therefore isolated from the bulk of the sample. Most of the sB synthesis experiments were

conducted using a bulk composition on a tie line between sB and H_2O. Three of the samples (1790, 1857, and 1875) contained four phases: A, sB, E, and H_2O (as evidenced by open pores). The E and A were found in segregations, either mixed together in crescent-shaped regions symmetric about the center of the capsule or individually in crescent-shaped bodies against the capsule wall. This type of phase separation in the presence of a fluid has been observed by others (Johnson and Walker 1993; Domanik and Holloway 1996) and is discussed in detail by Lesher and Walker (1988).

DISCUSSION

Although synthesis observations do not ensure that the phases represent thermodynamic equilibrium, the synthesis conditions can be used as a guide in the absence of other information. With the exception of the three samples discussed above and ignoring the occurrence of brucite and periclase as inclusions, the samples do not contain any textural evidence for disequilibrium. Most of our samples contained only three major phases, as is pre-

scribed by the phase rule. The phases are well mixed, and there is no textural evidence for reaction between them, such as embayment relationships or reaction rinds. Large temperature gradients can cause different assemblages to be stable in different parts of a capsule, creating confusion over which phases can be synthesized at a given temperature. Our samples appear homogeneous; no significant changes in phase relations or phase stability occurred over the range of temperatures experienced by a given sample. In the three samples in which phase separation occurred (1790, 1857, and 1875) we still interpret the presence of the phases to be indicative of their fundamental thermodynamic stability at the pressure-temperature conditions of the experiment. The phases are all well crystallized and do not display feathery or skeletal forms indicative of rapid crystallization on quench. We interpret the phase separation to indicate mass transport by the fluid in response to the temperature gradient. Here we discuss our synthesis results in the light of previous studies.

Phase A

Our synthesis observations suggest an extension of the pressure range for phase-A stability by several GPa (Fig. 3). Phase A was first synthesized by Ringwood and Major (1967). Yamamoto and Akimoto (1974, 1977) and Akimoto and Akaogi (1980) investigated its low-pressure stability limit. Yamamoto and Akimoto (1974) and Luth (1991, 1995) examined the stability of A in the presence of clinoenstatite. Using A as a starting material, Kanzaki (1991) investigated high-temperature (A = B + Br + H_2O) and high-pressure (A = F + aB + H_2O; aB = anhydrous B) decomposition reactions. Later, Kanzaki amended his observations (Kanzaki 1993), changing his identification of B at 14 GPa to sB and, at 17 GPa, including sB in the assemblage with aB and F. If we assume that the phases sB and aB are stoichiometric and that the fluid phase contains more H_2O than brucite, then neither the original high-pressure decomposition reaction nor the amended version can be written as a balanced equation; it is therefore not clear what the high-pressure decomposition reaction should be. We observed phase A in five experiments (1561, 1660, 1790, 1857, and 1875) at conditions above Kanzaki's high-temperature dehydration reactions [A = sB + Br + H_2O, A = B + Br + H_2O (Kanzaki 1991, 1993)]. Because these reactions involve the release of H_2O it is possible that the escape of H_2O from the capsule could alter their location. Of the five experiments, four were conducted in welded platinum and three contained open pores indicating the presence of water as a phase.

Phase B

Our synthesis observations of phase B also suggest a larger pressure-temperature stability range than previous work. B was first observed by Ringwood and Major (1967) and has since been observed in several studies (Akimoto and Akaogi 1980; Finger et al. 1989, 1991; Kanzaki 1991).

Akimoto and Akaogi (1980) investigated the low-pressure formation of B at 10 GPa. The high-temperature and high-pressure limits of B stability have not been systematically explored in any study to date. However, Kanzaki (1993) observed that sB replaced B as the breakdown product of A at 14 GPa and 1100 °C and observed the assemblage sB + aB at 17 GPa. He therefore proposed that B breaks down to aB + sB at conditions between 12 GPa, 1200 °C and 14 GPa, 1100 °C. We observed B at higher pressures and temperatures (Fig. 2). An alternative interpretation of Kanzaki's observations is that the formation of sB limits the bulk compositions at which B can form. Therefore, the appearance of sB as a decomposition product of A is more relevant to the low-pressure stability of sB than to the high-pressure stability of B, which does not break down to form aB + sB until higher pressures are reached. The data of Kato and Kumazawa (1985b, 1986) have not been included in this discussion or in Figure 2 because of the possible confusion of B with aB, which was unknown at that time (Finger et al. 1989).

Humite

The OH- and F-containing humites consist of a series of four naturally occurring phases. The OH end-members of two of these phases, chondrodite and clinohumite, have been found to have high-pressure stabilities. Our synthesis results suggest an extension to higher pressures of the stability fields of both these phases. Yamamoto and Akimoto (1974) identified OH–end-member chondrodite as phase D before it was correlated with natural chondrodite (Yamamoto 1977; Yamamoto and Akimoto 1977). Yamamoto and Akimoto (1977) and Akaogi and Akimoto (1980) investigated its phase stability (Fig. 4). Chondrodite is a common accessory phase in our synthesis experiments. Our data add a further constraint to the placement of the reaction A + forsterite = chondrodite that was previously investigated at pressures as high as 10 GPa (Akimoto and Akaogi 1980). Although the high-pressure limits of chondrodite stability have not been tested, the *P-T* slope of the reaction chondrodite = A + forsterite and the position of the solidus probably limit the high-pressure stability of chondrodite to <16–17 GPa.

Clinohumite stability has also been explored (Yamamoto and Akimoto 1977; Akaogi and Akimoto 1980) (Fig. 5) and is similar to that of chondrodite (Fig. 4), but clinohumite was thought to break down to chondrodite + forsterite above about 8 GPa (Akaogi and Akimoto 1980). Clinohumite formed in only a few of our synthesis experiments. At 1000 °C and 12 GPa we observed forsterite coexisting with A (expt. 1669), which, if in equilibrium, would indicate that clinohumite was not stable there. Two of our samples synthesized at 12 GPa, 1154 and 1158 °C (expts. 1747 and 1752, respectively) contained both chondrodite and forsterite. Although we did not find chondrodite and forsterite in grain-to-grain contact, a region of forsterite-chondrodite coexistence is shown with dashed lines in Figure 5. Because very small variations in local bulk composition could account for

these observations, they do not conclusively demonstrate that clinohumite is unstable at those conditions. Our synthesis observations of clinohumite fall on either side of the extension of the reaction clinohumite = forsterite + A, identified at lower pressure (Yamamoto and Akimoto 1977), but well above the placement of the reaction clinohumite = chondrodite + forsterite proposed by Akimoto and Akaogi (1980). Kanzaki (1991) also observed clinohumite at similar pressures but at lower temperature, virtually the same temperature at which we observed Phase A + forsterite. These results indicate that the high-pressure stability of clinohumite may extend beyond 8 GPa and should be further examined. This is particularly important because monolayers of Ti-bearing clinohumite have been identified in olivine from the Buell Park kimberlites (Kitamura et al. 1987), suggesting that this may be a naturally occurring mechanism for water storage in the upper mantle.

There appear to be persistent inconsistencies between our results and those of Kanzaki (1991, 1993). For example, Kanzaki's experimental data plotted in Figures 2, 3, and 5 would need to be shifted to higher temperature by about 100 °C to be consistent with our results. This may be largely due to a combination of experimental uncertainty and the effects of pressure on the various thermocouples used. Kanzaki noted that his sample assembly resulted in a heterogeneous temperature distribution of up to 100 °C across the sample; this may have led to a similar uncertainty in the temperature assignments to synthesis conditions. Temperature gradients in our cell are less steep (approximately 15°/mm; Gwanmesia and Liebermann 1992), and with the exception of the three experiments discussed above (1790, 1857, and 1875) there was no petrologic evidence for a temperature gradient across the samples. Kanzaki used Pt/Pt13%Rh thermocouples, whereas we used W3%Re vs. W25%Re alloy (type D). The effect of pressure on emf was not corrected for in either study because the absolute effect is not well known. The relative effect between these two types of thermocouples has been studied (Ohtani et al. 1982; Kato and Kumazawa 1985a; Walter et al. 1995), and it has been found that Pt/Pt13%Rh thermocouples read low compared with W-Re alloy thermocouples. Walter et al. (1995) measured a difference of 20–30 °C over similar pressure-temperature conditions. The difference is also a function of the temperature at the pressure seal (see Luth 1993), which varies from assembly to assembly. An increase in Kanzaki's experimental temperatures of about 100 °C, or in some cases a smaller temperature increase combined with a pressure increase, would eliminate much of the difference between the two studies.

Phase C

Phase C was not observed in this study, however, its absence is noteworthy. C was first identified by Ringwood and Major (1967) on the basis of X-ray reflections. It was observed in experiments with bulk compositions that had >5% H_2O and Mg/Si ratios between 3 and 5. Ringwood

and Major did not specify which pressure and temperature conditions produced phase C, but their experiments were all conducted between 600 and 1100 °C and 10 and 18 GPa. Akaogi and Akimoto (1980) reported the occurrence of phase C between 13 and 16 GPa and 800 and 1000 °C in experiments that also produced phases A and B, β-Mg_2SiO_4, and periclase. Their identification of phase C was made on the basis of peaks in the X-ray powder pattern. Our A and sB bulk-composition starting mixtures and experimental conditions fall within the range of those identified by Ringwood and Major (1967) and Akaogi and Akimoto (1980); therefore, we expected to see C in our experiments. However, we saw no evidence of phases other than those already identified. Kanzaki (1993) proposed that sB is in fact C. If this is the case, our experimental results are in agreement with the work of Ringwood and Major (1967) and Akaogi and Akimoto (1980). Gasparik (1993) identified C on the basis of microprobe analysis, assigning it a variable Mg/Si ratio of 2.9–3.5. At the conditions at which Gasparik identified C (9–12 GPa, 1000–1200 °C) we observed only phases A and B, forsterite, clinohumite, and chondrodite. Because most of the composition space that Gasparik assigned to C lies within the composition space we investigated, we suggest that the phase identified as C by Gasparik (1993) is either clinohumite or chondrodite, neither of which was seen by Gasparik in the pressure-temperature-composition space where they are known to form. In addition, both of these phases are prone to damage under the electron beam and tend to yield variable analyses.

Phase coexistence

There are nine known hydrous phases in the MgO-SiO_2-H_2O system with significant high-pressure stabilities. Using these phases in combination with the anhydrous phases and fluid, one can construct a petrogenetic grid with well over 1000 reactions. Although only a limited portion of the grid occupies regions of pressure-temperature space that are of relevance to the Earth's mantle, there are still many reactions to be investigated. However, some reactions would play a more critical role than others in the subduction and storage of H_2O in the mantle. By observing which phases coexist at relevant pressures and temperatures, we can begin to develop a sense of what these important reactions are.

The observation of the coexistence of phases in synthesis experiments does not guarantee their mutual participation in true equilibrium assemblages, but it does offer a place to start evaluating which reactions are likely to be important. Because the majority of the samples contain homogeneous, well-mixed, three-phase assemblages, this use of our observations is not unreasonable. Figure 6 contains four compositional plots showing tie lines that represent the grain-to-grain contacts, and contacts between inclusions and their host grains, that were documented in the synthesis experiments.

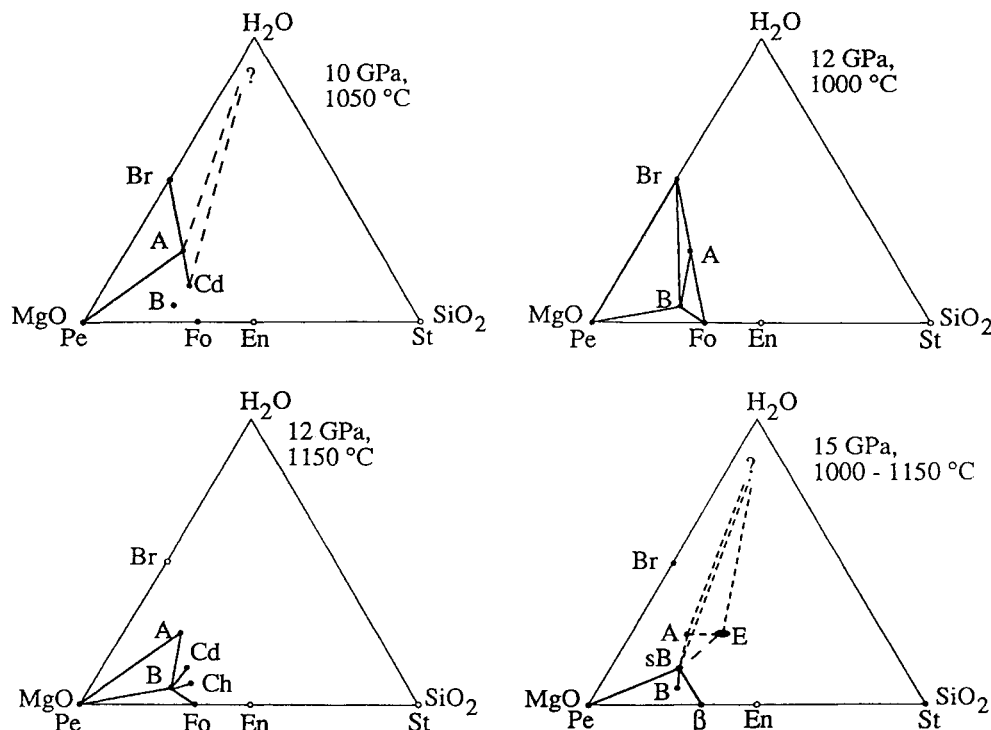An important reaction that limits the pressure and temperature conditions at which A is stable in mantle

FIGURE 6. Compositional plots of the MgO-SiO$_2$-H$_2$O system showing tie lines observed at 10 GPa and 1050 °C, 12 GPa and 1000 °C, 12 GPa and 1150 °C, and 15 GPa and 1000–1150 °C. Solid circles indicate phases present. Solid tie lines represent observed grain-to-grain contacts. Dashed tie lines to H$_2$O (composition of fluid unknown) are inferred from the presence of porosity. Dashed tie lines at 15 GPa are proposed on the basis of textures in four-phase samples.

rocks is: A + En = Fo + fl. Luth (1991, 1995) observed this reaction between 860 and 880 °C at 9 GPa. At 10 GPa and 1050 °C we observe open porosity in specimens that contain A and chondrodite and infer the presence of water in the specimen (expts. 1783, 1794, and 1830). The tie lines between A and water and between chondrodite and water are shown as dashed because the water was not observed directly. These tie lines are consistent with the observation that the tie line between A and enstatite breaks down at lower temperature in favor of forsterite and water.

Although it has been proposed that phase B could be a significant carrier of H$_2$O into the mantle (Finger et al. 1989), it now appears, owing to the high-pressure stability of humite and phase A, that B is not likely to form in mantle compositions. At 12 GPa and 1000 °C (expt. 1669) we observed the coexistence of A and forsterite, consistent with previous studies (Yamamoto and Akimoto 1977; Akaogi and Akimoto 1980). At 12.4 GPa and 1154 °C we observed a three-phase assemblage containing B, forsterite, and chondrodite. Both chondrodite and forsterite are minor phases, and so we were not able to find two grains touching each other; however, it seems likely that they can coexist. Both the tie line between A and forsterite and that between chondrodite and forsterite isolate B from mantle compositions. At 12 GPa and 1150 °C (expts. 1729 and 1864) we observed that clinohumite is stable;

a tie line between clinohumite and forsterite would have the same effect.

The formation of sB and phase E accompanies an important shift in the topology of tie lines on the compositional plot. Tie lines between A and B and periclase do not necessitate the absence of sB at 12 GPa; however, they severely limit the region of compositional space in which assemblages containing sB can occur. With increasing pressure between 12 and 15 GPa, sB appears [consistent with Kanzaki's (1991, 1993) observations] and a series of reactions occur, including B + A = sB + β-Mg$_2$SiO$_4$. The tie lines between B and the two humites would also necessarily be broken by the tie line between sB and β-Mg$_2$SiO$_4$. However, the reactions clinohumite = forsterite + chondrodite and chondrodite = A + forsterite may well take place before sB forms. The most important reactions involving sB are those that allow it to coexist with phases that are more Si rich than forsterite because these reactions break the tie line between forsterite and H$_2$O. In three of our experiments (1790, 1857, and 1875) we observed sB coexisting with phase E. However, these results must be interpreted with caution because the presence of four phases in experiments and the segregation of the phases into distinct regions clearly indicate that these samples were not in equilibrium. The phase separation suggests mass transport by the fluid in response to temperature gradients. The pressure-temper-

ature conditions of these experiments are at and above the high-temperature dehydration reaction of sB + stishovite as reported by Gasparik (1993). Therefore, it could be inferred that sB is not stable above approximately 1100 °C at these pressures. However, at the same conditions sB was synthesized in the presence of B and no excess water (expt. 1881), and the sample showed no textural evidence for dehydration. Therefore, the best interpretation is that in some portions of these samples the sB-to-H_2O tie line was broken in favor of a tie line between A and E. These ties lines are shown in Figure 6 as dashed. The tendency for phase separation at conditions near a reaction boundary in experiments with excess water was also observed by Domanik and Holloway (1996). The tie lines from sB to H_2O and from sB to E break the tie lines between A and β-Mg_2SiO_4, removing any possibility that A could participate in mantle assemblages once sB has formed. The tie lines between E and either sB or A also preclude the coexistence of β-Mg_2SiO_4 and water. This geometry is consistent with the observation that sB can coexist with stishovite under some conditions (Gasparik 1993; Pacalo and Parise 1992). It is the behavior of the forsterite + H_2O tie line over all others that determines to what degree the dense high-pressure magnesium silicates are present in the mantle.

The textures in our samples indicate that the presence of water as a free fluid phase has a strong effect on grain size. Although there is some variation between experiments in which water was not present as a free phase but was crystallographically bound as H, these experiments have smaller grain sizes, similar to those in a completely anhydrous experiment. Grains of the same phase may be ten times larger in experiments where water is present as a free phase. This observation lends weight to the speculation that the release of H_2O produced by dehydration reactions in down-going slabs may flux diffusion-dependent processes as it is known to do at shallower depths.

REFERENCES CITED

Akaogi, M., and Akimoto, S.-i. (1980) High-pressure stability of a dense hydrous magnesian silicate $Mg_{23}Si_8O_{42}H_6$ and some geophysical implications. Journal of Geophysical Research, 85, 6944–6948.

Akimoto, S., and Akaogi, M. (1980) The system Mg_2SiO_4-MgO-H_2O at high pressures and temperatures: Possible hydrous magnesian silicates in the mantle transition zone. Physics of Earth and Planetary Interiors, 23, 268–275.

Bell, D.R., and Rossman, G.R. (1992) Water in Earth's mantle: The role of nominally anhydrous minerals. Science, 255, 1391–1397.

Burnley, P.C. (1995) The fate of olivine in subducting slabs: A reconnaissance study. American Mineralogist, 80, 1293–1301.

Domanik, K.J., and Holloway, J.R. (1996) The stability and composition of phengitic muscovite and associated phases at 5.5–10 GPa: Implications for deeply subducted sediments. Geochimica et Cosmochemica Acta, in press.

Finger, L.W., Ko, J., Hazen, R.M., Gasparik, T., Hemley, R.J., Prewitt, C.T., and Weidner, D.J. (1989) Crystal chemistry of phase B and an anhydrous analogue: Implications for water storage in the upper mantle. Nature, 341, 140–142.

Finger, L.W., Hazen, R.M., and Prewitt, C.T. (1991) Crystal structures of $Mg_{12}Si_4O_{19}(OH)_2$ (phase B) and $Mg_{14}Si_5O_{24}$ (phase AnhB). American Mineralogist, 76, 1–7.

Gasparik, T. (1990) Phase relations in the transition zone. Journal of Geophysical Research, 95, 15751–15769.

———(1993) The role of volatiles in the transition zone. Journal of Geophysical Research, 98, 4287–4299.

Gwanmesia, G.D., and Liebermann, R.C. (1992) Polycrystals of high pressure phases of mantle minerals: Hot-pressing and characterization of physical properties. In Y. Syono and M.H. Manghnani, Eds., High pressure research in mineral physics: Application to earth and planetary sciences, p. 117–135. American Geophysical Union, Washington, DC.

Gwanmesia, G.D., Li, B., and Liebermann, R.C. (1993) Hot pressing of polycrystals of high-pressure phases of mantle minerals in multi-anvil apparatus. Pageoph, 141, 467–484.

Horiuchi, H., Morimoto, N., Yamamoto, K., and Akimoto, S. (1979) Crystal structure of $2Mg_2SiO_4 \cdot 3Mg(OH)_2$, a new high-pressure structure type. American Mineralogist, 64, 593–598.

Inoue, T., Yurimoto, H., and Kudoh, Y. (1995) Hydrous modified spinel, $Mg_{1.75}SiH_{0.5}O_4$: A new water reservoir in the mantle transition region. Geophysical Research Letters, 22(2), 117–120.

Johnson, M.C., and Walker, D. (1993) Brucite [$Mg(OH)_2$] dehydration and the molar volume of H_2O to 15 GPa. American Mineralogist, 78, 271–284.

Kanzaki, M. (1991) Stability of hydrous magnesium silicates in the mantle transition zone. Physics of the Earth and Planetary Interiors, 66, 307–312.

———(1993) Calculated powder X-ray patterns of phase B, anhydrous B and superhydrous B: Re-assessment of previous studies. Mineralogical Journal, 16(5), 278–285.

Kato, T., and Kumazawa, M. (1985a) Effect of high pressure on the melting relation in the system Mg_2SiO_4-$MgSiO_3$: Part 1. Eutectic relation up to 7 GPa. Journal of the Physics of the Earth, 33, 513–524.

———(1985b) Stability of phase B, a hydrous magnesium silicate, to 2300 °C at 20 GPa. Geophysical Research Letters, 12, 534–535.

———(1986) Melting experiment on natural lherzolite at 20 GPa: Formation of phase B coexisting with garnet. Geophysical Research Letters, 13, 181–184.

Kitamura, M., Kondoh, S., Morimoto, N., Miller, G.H., Rossman, G.R., and Putnis, A. (1987) Planar OH-bearing defects in mantle olivine. Nature, 328, 143–145.

Kudoh, Y., Finger, L.W., Hazen, R.M., Prewitt, C.T., Kanzaki, M., and Veblen, D.R. (1993) Phase E: A high pressure hydrous silicate with a unique crystal chemistry. Physics and Chemistry of Minerals, 19, 357–360.

Lesher, C.E., and Walker, D. (1988) Cumulate maturation and melt migration in a temperature gradient. Journal of Geophysical Research, 93, 10295–10311.

Liu, L.-g. (1987) Effects of H_2O on the phase behavior of the forsterite-enstatite system at high pressures and temperatures and implications for the Earth. Physics of the Earth and Planetary Interiors, 49, 142–167.

Luth, R.W. (1991) Stability of phase A in the Earth's mantle. Eos, 72(44), 499.

———(1993) Measurement and control of intensive parameters in experiments at high pressure in solid-media apparatus. In R. Luth, Ed., Mineralogical association of Canada short course handbook on experiments at high pressure and applications to the Earth's mantle, p. 15–37. Mineralogical Association of Canada, Napean, Ontario.

———(1995) Is phase A relevant to the Earth's mantle? Geochimica et Cosmochimica Acta, 59, 679–682.

Meade, C., and Jeanloz, R. (1991) Deep-focus earthquakes and recycling of water into the Earth's mantle. Science, 252, 68–72.

Ohtani, E., Kumazawa, E., Kato, M., and Irifune, T. (1982) Melting of various silicates at elevated pressures. In S. Akimoto and M.H. Manghnani, Eds., High-pressure research in geophysics, p. 259–269. Center of Academic Publications, Tokyo.

Pacalo, R.E.G., and Parise, J.B. (1992) Crystal structure of superhydrous B, a hydrous magnesium silicate synthesized at 1400 °C and 20 GPa. American Mineralogist, 77, 681–684.

Pawley, A.R. (1994) The pressure and temperature stability of lawsonite: Implications for H_2O recycling in subduction zones. Contributions to Mineralogy and Petrology, 118, 99–108.

Peacock, S.M. (1990) Fluid processes in subduction zones. Science, 248, 329–337.

Raleigh, C.B., and Paterson, M.S. (1965) Experimental deformation of serpentinite and its tectonic implications. Journal of Geophysical Research, 70(16), 3965–3985.

Ringwood, A.E., and Major, A. (1967) High-pressure reconnaissance investigations in the system Mg_2SiO_4-MgO-H_2O. Earth and Planetary Science Letters, 2, 130–133.

Selverstone, J., Franz, G., Thomas, S., and Getty, S. (1992) Fluid variability in 2 GPa eclogites as an indicator of fluid behavior during subduction. Contributions to Mineralogy and Petrology, 112, 341–357.

Smyth, J.R. (1994) A crystallographic model for hydrous wadsleyite (β-Mg_2SiO_4): An ocean in the Earth's interior? American Mineralogist, 79, 1021–1024.

Smyth, J.R., Swope, R.J., and McCormick, T.C. (1991) Crystal chemistry of hydrous clinopyroxenes from the mantle. Eos, 72(44), 499.

Sudo, A., and Tatsumi, Y. (1990) Phlogopite and K-amphibole in the upper mantle: Implication for magma genesis in subduction zones. Geophysical Research Letters, 17(1), 29–32.

Trønnes, R.G. (1990) Low-Al, high-K amphiboles in subducted lithosphere from 200 to 400 km depth: Experimental evidence. Eos, 71(43), 1587.

Trønnes, R.G., Takahashi, E., and Scarfe, C.M. (1988) Stability of K-richterite and phlogopite to 4 GPa. Eos, 69(44), 1510–1511.

Walter, M., Thibault, Y., Wei, K., and Luth, R.W. (1995) Characterizing pressure and temperature conditions in experiments in multi-anvil apparatus. Canadian Journal of Physics, 73, 273–286.

Wunder, B., and Schreyer, W. (1992) Metastability of the 10-Å phase in the system MgO-SiO_2-H_2O (MSH): What about hydrous MSH phases in subduction zones? Journal of Petrology, 33(4), 877–889.

Yamamoto, K. (1977) The crystal structure of hydroxyl-chondrodite. Acta Crystallographica, B33, 1481–1486.

Yamamoto, K., and Akimoto, S.-i. (1974) High pressure and high temperature investigations in the system MgO-SiO_2-H_2O. Journal of Solid State Chemistry, 9, 187–195.

——— (1977) The system MgO-SiO_2-H_2O at high pressures and high temperatures: Stability field for hydroxyl-chondrodite, hydroxyl-clinohumite, and 10 Å-phase. American Journal of Science, 277, 288–312.

Young, T.E., Green, H.W.I., and Hofmeister, A.M. (1991) OH solubility and speciation in β-$(Mg,Fe)_2SiO_4$. Eos, 72, 144.